J|A|C|S ARTICLES

Published on Web 03/25/2010

In Situ Misfolding of Human Islet Amyloid Polypeptide at Interfaces Probed by Vibrational Sum Frequency Generation

Li Fu, Gang Ma, and Elsa C. Y. Yan*

Department of Chemistry, Yale University, 225 Prospect Street, New Haven, Connecticut 06520

Received November 10, 2009; E-mail: elsa.yan@yale.edu

Abstract: Kinetic analysis of conformational changes of proteins at interfaces is crucial for understanding many biological processes at membrane surfaces. In this study, we demonstrate that surface-selective sum frequency generation (SFG) spectroscopy can be used to investigate kinetics of conformational changes of proteins at interfaces. We focus on an intrinsically disordered protein, human islet amyloid polypeptide (hIAPP) that is known to misfold into the β-sheet structure upon interaction with membranes. Using the ssp polarization setting (s-polarized SFG, s-polarized visible, and p-polarized infrared), we observe changes in the amide I spectra of hIAPP at the air/water interface after addition of dipalmitoylphosphoglycerol (DPPG) that correspond to the lipid-induced changes in secondary structures. We also used the chiral-sensitive psp polarization setting to obtain amide I spectra and observed a gradual buildup of the chiral structures that display the vibrational characteristics of parallel β-sheets. We speculate that the second-order chiral-optical response at the antisymmetric stretch frequency of parallel β-sheet at 1622 cm^{-1} could be a highly characteristic optical property of the β-sheet aggregates not only for hIAPP, but possibly also for other amyloid proteins. Analyzing the achiral and chiral amide I spectra, we conclude that DPPG induces the misfolding of hIAPP from α-helical and random-coil structures to the parallel β-sheet structure at the air/water interface. We propose that SFG could complement existing techniques in obtaining kinetic and structural information for probing structures and functions of proteins at interfaces.

Introduction

Kinetic analysis of conformational changes of proteins at interfaces is important for understanding numerous biological phenomena at membrane surfaces, such as signal transduction,[1] cell adhesion,[2] and active molecular transport across membranes.[3] In this study, we show that surface-selective sum frequency generation (SFG) spectroscopy can be used to investigate conformational changes of proteins at interfaces. We focus on an intrinsically disordered protein, human islet amyloid polypeptide (hIAPP) that is known to aggregate into β-sheet structures when it interacts with lipid membranes. Using SFG, we observe time-dependent spectral changes in the amide I region corresponding to the misfolding of hIAPP induced by dipalmitoylphosphoglycerol (DPPG) at the air/water interface. We also find that the lipid-induced misfolded structures of hIAPP display chirality with the vibrational characteristics of parallel β-sheet structures. Our results demonstrate the utility of SFG for studying kinetics of conformational changes of proteins at interfaces.

Human islet amyloid polypeptide consists of 37 amino acids and belongs to the family of intrinsically disordered proteins. This family of proteins is unstructured in solution, but folds into more ordered structures upon binding to their interacting partners.[4,5] They have gained tremendous attention because their misfolding is related to disorders such as Alzheimer's disease, Parkinson's disease, and type II diabetes.[6−8] In particular, hIAPP is associated with type II diabetes.[9] In the normal state, hIAPP is cosecreted with insulin from the islet β-cells of the pancreas, and adopts an unstructured conformation. In the disease state, hIAPP misfolds into amyloid aggregates deposited in the islet cells of pancreas and leads to the death of the β-cells, which produce insulin.[9] Intriguingly, rat islet amyloid polypeptide (rIAPP), which differs from hIAPP only by six amino acids, does not fold into the β-sheet aggregates, and rats do not suffer from type II diabetes.[10] A fundamental understanding of the molecular interactions between hIAPP and lipid membranes as well as the subsequent misfolding of hIAPP is necessary to reveal the molecular pathology of type II diabetes.[11−13]

Many efforts have been devoted to elucidating the structural details of the misfolding process of hIAPP using a variety of

(1) Palczewski, K.; Kumasaka, T.; Hori, T.; Behnke, C. A.; Motoshima, H.; Fox, B. A.; Le Trong, I.; Teller, D. C.; Okada, T.; Stenkamp, R. E.; Yamamoto, M.; Miyano, M. *Science* **2000**, *289*, 739–745.
(2) Keselowsky, B. G.; Collard, D. M.; Garcia, A. J. *J. Biomed. Mater. Res., Part A* **2003**, *66A*, 247–259.
(3) Higgins, C. F. *Annu. Rev. Cell Dev. Biol.* **1992**, *8*, 67–113.
(4) Hopener, J. W. M.; Lips, C. J. M. *Int. J. Biochem. Cell Biol.* **2006**, *38*, 726–736.
(5) Kahn, S. E.; Andrikopoulos, S.; Verchere, C. B. *Diabetes* **1999**, *48*, 241–253.
(6) Dyson, H. J.; Wright, P. E. *Nat. Rev. Mol. Cell Biol.* **2005**, *6*, 197–208.
(7) Tompa, P. *Trends Biochem. Sci.* **2002**, *27*, 527–533.
(8) Uversky, V. N. *Protein Sci.* **2002**, *11*, 739–756.
(9) Chiti, F.; Dobson, C. M. *Annu. Rev. Biochem.* **2006**, *75*, 333–366.
(10) Westermark, P.; Engstrom, U.; Johnson, K. H.; Westermark, G. T.; Betsholtz, C. *Proc. Natl. Acad. Sci. U.S.A.* **1990**, *87*, 5036–5040.
(11) Engel, M. F. M. *Chem. Phys. Lipids* **2009**, *160*, 1–10.
(12) Brender, J. R.; Lee, E. L.; Cavitt, M. A.; Gafni, A.; Steel, D. G.; Ramamoorthy, A. *J. Am. Chem. Soc.* **2008**, *130*, 6424–6429.
(13) Jayasinghe, S. A.; Langen, R. *Biochim. Biophys. Acta, Biomembr.* **2007**, *1768*, 2002–2009.

spectroscopic techniques. Jefferson et al. used circular dichroism (CD) spectroscopy and observed that hIAPP adopts a random-coil structure in solution but folds into β-sheets upon binding to liposomes made of 1,2-dioleoyl-sn-glycero-3-(phospho-rac-1-glycerol) (DOPG).[14] Sajith et al. performed thioflavin T fluorescence assay with hIAPP and observed that its fluorescence increases after addition of the negatively charged phosphatidylserine liposomes into the hIAPP solution, suggesting that aggregation of hIAPP is triggered by the presence of the lipid membranes.[15] Moreover, Zanni and co-workers studied hIAPP by two-dimensional infrared spectroscopy (2D-IR) both in the presence and absence of negatively charged lipid vesicles consisting of 1,2-dioleoyl-sn-glycero-3-phosphate (DOPA) and 1,2-dio-leoyl-sn-glycero-3-phosphocholine (DOPC).[16] They found that lipid membranes dramatically expedite the kinetics of the aggregation of hIAPP. They also observed a characteristic spectral feature of the β-sheet during membrane-mediated aggregation of hIAPP. In addition, the Winter group used infrared reflection absorption spectroscopy (IRRAS) to study hIAPP aggregation at the air/water interface in the presence and absence of 1-palmitoyl-2-oleoyl-sn-2-glycero-3-phosphocholine (POPG).[17] They observed that the amide I band of hIAPP is centered at $\sim$1625 cm^{-1} after addition of POPG and concluded that the misfolded structures of hIAPP consist of parallel β-sheet structures. Finally, Tycko and co-workers examined the structures of hIAPP fibrils using solid-state NMR.[18] They performed the experiments on a series of isotopically labeled peptides and concluded that the aggregated fibrils consist of layers of parallel β-sheets with a C_2 symmetric arrangement. All these spectroscopic studies suggest that the interactions between lipid membranes and hIAPP trigger the misfolding of hIAPP. The results have led to a working model that hIAPP initially forms the α-helical structure upon adsorption on membrane surfaces and then cooperatively converts into β-sheet aggregates.[13,14]

Because previous biophysical studies have established that hIAPP, but not rIAPP, can aggregate into β-sheet-rich structures and that this aggregation process is triggered by interactions with lipid molecules, the IAPP system is an excellent model to demonstrate the applicability of SFG for investigating kinetics of protein folding or misfolding at interfaces. By monitoring the amide I spectra of hIAPP and rIAPP in the presence and absence of lipid molecules at the air/water interface, we can establish control experiments that allow us to correlate the SFG spectra in the amide I region to the conformational changes in hIAPP and rIAPP upon interactions with lipid molecules.

Over the past two decades, SFG has been developed into a powerful surface specific technique to solve problems in physical, material, and environmental sciences.[19] In recent years, it has been extended to the investigation of biological molecules at interfaces. Pioneering works include protein adsorption at various surfaces,[20] flip/flop kinetics of lipid molecules in biomembranes,[21] and chirality of DNA on solid substrates.[22] As a second-order optical technique, SFG utilizes one visible laser beam and one infrared (IR) laser beam, which interact with the molecules at interface and generate a third beam at the sum freqeuncy of the visible and IR beams. When the IR input frequency is in resonance with an interfacial vibrational mode, the SFG beam can be enhanced. Therefore, SFG is sensitive to vibrational structure. SFG is known for its surface-sensitivity that originates from the selection rule of the second-order optical process. Under dipole approximation, SFG is allowed at noncentrosymmetric interfaces, but forbidden in centrosymmetric bulk media.[23] To study protein conformation at interfaces, SFG can be used to probe the amide I vibration structures. Because the amide I vibration is sensitive to the secondary structure (e.g., α-helix, β-sheet, etc.),[24] SFG is a label-free method for probing the folding and misfolding of proteins. In probing the amide I vibrational modes in the region of 1600$-$1700 cm^{-1}, SFG can be free of background from the bending mode of H_2O as demonstrated in our experiments using the ssp (s-polarized sum frequency beam, s-polarized visible beam, and p-polarized IR beam) and psp polarizations. Moreover, by using the chiral-sensitive psp polarization, SFG can be used to probe the chirality of vibrational structures of proteins, which is particularly useful for probing the molecular assembling processes of protein complexes.

Applying SFG to probe hIAPP at the air/water interface, we made two important observations. First, we observed a time-dependent spectral shift in the amide I region that reveal kinetics of protein conformational changes at interfaces. Using the ssp polarization, we observed that introduction of the negatively charged DPPG triggers a spectral shift in the amide I spectrum of hIAPP, but not that of rIAPP, which is in good agreement with the current understanding that lipids can induced misfolding of hIAPP, but not rIAPP. Second, we used the chiral-sensitive psp polarization and did not observe any chiral SFG signal from hIAPP at the air/water interface. However, upon addition of DPPG, we observed a gradual increase of the chiral signal centered at $\sim$1620 cm^{-1}, which is highly characteristic of the antisymmetric stretch of the parallel β-sheet. This observed chiral SFG could be a highly characteristic second-order optical response not only from the hIAPP aggregate, but possibly from other amyloid proteins as well. We speculate, on the basis of the theory developed by Simpson and co-workers, that the chiral SFG signal from misfolded hIAPP is originated from the chiral orientation of individual peptides in the aggregates. Combining the results of the achiral and chiral SFG measurements, we demonstrate that SFG is an *in situ* technique able to yield both kinetic and structural information about conformational changes of proteins at interfaces.

Experimental Section

SFG Setup. The SFG setup was described in detail in Ma et al.[25] Briefly, it consists of a 6-W regenerative amplifier (<120 fs) seeded by a Ti:sapphire oscillator and pumped by two Nd:YLF lasers. One half of the 6-W output from the amplifier

(14) Knight, J. D.; Hebda, J. A.; Miranker, A. D. *Biochemistry* **2006**, *45*, 9496–9508.
(15) Jayasinghe, S. A.; Langen, R. *Biochemistry* **2005**, *44*, 12113–12119.
(16) Ling, Y. L.; Strasfeld, D. B.; Shim, S. H.; Raleigh, D. P.; Zanni, M. T. *J. Phys. Chem. B* **2009**, *113*, 2498–2505.
(17) Lopes, D. H. J.; Meister, A.; Gohlke, A.; Hauser, A.; Blume, A.; Winter, R. *Biophys. J.* **2007**, *93*, 3132–3141.
(18) Luca, S.; Yau, W.-M.; Leapman, R.; Tycko, R. *Biochemistry* **2007**, *46*, 13505–13522.
(19) Wang, H. F.; Gan, W.; Lu, R.; Rao, Y.; Wu, B. H. *Int. Rev. Phys. Chem.* **2005**, *24*, 191–256.
(20) Wang, J.; Buck, S. M.; Chen, Z. *J. Phys. Chem. B* **2002**, *106*, 11666–11672.
(21) Anglin, T. C.; Liu, J.; Conboy, J. C. *Biophys. J.* **2007**, *92*, L1–L3.
(22) Stokes, G. Y.; Gibbs-Davis, J. M.; Boman, F. C.; Stepp, B. R.; Condie, A. G.; Nguyen, S. T.; Geiger, F. M. *J. Am. Chem. Soc.* **2007**, *129*, 7492–7493.
(23) Shen, Y. R. *Nature* **1989**, *337*, 519–525.
(24) Barth, A.; Zscherp, C. *Q. Rev. Biophys.* **2002**, *35*, 369–430.
(25) Ma, G.; Liu, J.; Fu, L.; Yan, E. C. Y. *Appl. Spectrosc.* **2009**, *63*, 528–537.

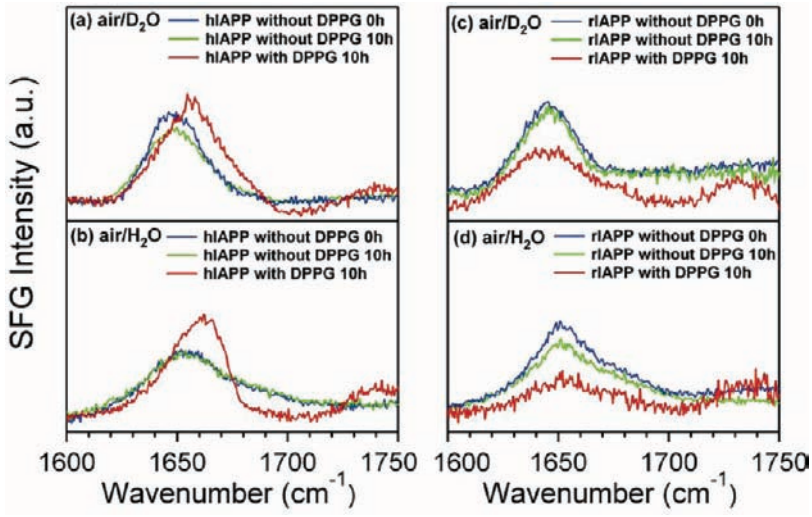

Figure 1. The ssp spectra of hIAPP without DPPG ($t = 0$ h and $t = 10$ h) and at $t = 10$ h after addition of DPPG at the (a) air/D_2O and (b) air/H_2O interfaces. The ssp spectra of rIAPP without DPPG ($t = 0$ h and $t = 10$ h) and at $t = 10$ h after addition of DPPG rIAPP at the (c) air/D_2O and (d) air/H_2O interfaces.

passed through a home-built pulse shaper to produce narrow-bandwidth 800-nm pulses with a bandwidth of 7 cm^{-1}, and the other half of the output pumped an automated optical parametric amplifier (OPA) to generate broad-bandwidth IR pulses. The power of the 800-nm beam at the sample stage was ~135 mW, and the power of the OPA output at the sample stage was ~10 mW. The incident angles for the 800-nm and IR beams were 56° and 69°, respectively. The SFG signal generated from the sample was filtered and then dispersed by a monochromator before being detected by a CCD.

Materials and Sample Preparation. The DPPG lipid was purchased from Avanti Polar lipids as powder and dissolved in chloroform. The hIAPP and rIAPP samples were synthesized and purified by the W.M. Keck Facility at Yale University. The lyophilized hIAPP and rIAPP were dissolved in deionized water, and the concentration was determined by UV absorbance. The solutions of the peptides were distributed into vials, which were frozen in liquid nitrogen and stored at −80 °C. Each vial of the solution was thawed for one SFG experiment and never frozen again.

Experimental Procedure and Data Acquisition. In the SFG experiments, a Teflon beaker containing 4 mL of phosphate buffer (10 mM phosphate, pH/pD = 7.4) was placed on the sample stage. A solution of hIAPP or rIAPP at a concentration of ~100 μM was added using a microsyringe to give the final concentration of 1 μM. The total amount of the sample used for each measurement was ~4 μg. The SFG signal from the air/water interface was monitored after addition of hIAPP or rIAPP. The DPPG lipid was added as a solution in chloroform using a microsyringe at a surface coverage of 107 $Å^2$ per molecule. After the addition of DPPG, one or two SFG spectra were taken every hour to monitor the spectral changes, and the whole process was monitored for ~10 h. The acquisition time for each spectrum was 10 min. To avoid evaporation of the solution, the beaker was covered with a plastic cap between acqusitions of spectra. By adjusting the polarizer in front of the monochromator, the SFG spectra were taken alternately using the ssp or psp polarizations.

Processing and Analysis of Data. The raw spectra were processed as described in Ma et al.,[25] including the steps of removing the contribution from cosmic rays, subtracting background, calibrating the wavenumber, and normalizing to the IR power. To analyze the secondary structures of the peptides, the processed spectra were analyzed using eq 1

$$I_{SFG} \propto \left| \chi_{NR}^{(2)} + \sum_q \frac{A_q}{\omega_{IR} - \omega_q + i\Gamma_q} \right|^2 \qquad (1)$$

where I_{SFG} is the sum frequency intensity, χ_{NR} is the nonresonant second-order susceptibility, ω_{IR} is the input IR frequency, and A_q, ω_q, and Γ_q are the amplitude, resonant frequency, and damping factor of the qth vibration mode, respectively.

Results

We monitored the SFG spectra in the amide I region of hIAPP and rIAPP in the presence and absence of DPPG at the air/H_2O and D_2O interfaces using the ssp and psp polarizations to investigate the lipid-induced misfolding process of hIAPP. Results are presented in Figures 1−3.

Figure 1 presents the initial and final amide I spectra of hIAPP and rIAPP taken using the ssp polarization at the air/H_2O and D_2O interfaces in the absence of DPPG at $t = 0$ and ~10 h and in the presence of DPPG at $t \approx 10$ h after addition of DPPG. Figure 1a,b shows the amide I bands of hIAPP centered at ~1650 cm^{-1} at the air/D_2O and air/H_2O interfaces in the absence of DPPG, suggesting that hIAPP adsorbs at the interfaces. The position and shape of the peaks remain unchanged over 10 h, indicating that hIAPP is stable at the air/water interfaces. The change of intensity of the peaks could be due to evaporation of solvent and/or fluctuation of laser power. After addition of DPPG, a peak appears at 1735 cm^{-1} (Figure 1 a,b), which is due to the carbonyl groups of DPPG. Also, the amide I peak undergoes changes in both shape and position after the addition of DPPG. These changes are not observed in the absence of DPPG. The results suggest that DPPG induces secondary structural changes in hIAPP. Figure 1 c,d presents the amide I spectra of rIAPP at both the air/H_2O and air/D_2O interface. The spectra do not change over 10 h in the absence of DPPG, indicating that rIAPP also adsorbs and is stable at the air/water interface. Upon addition of DPPG, although the intensity of the amide I band changes probably due to evaporation of solvent and/or fluctuation of laser power, the shape and position of the

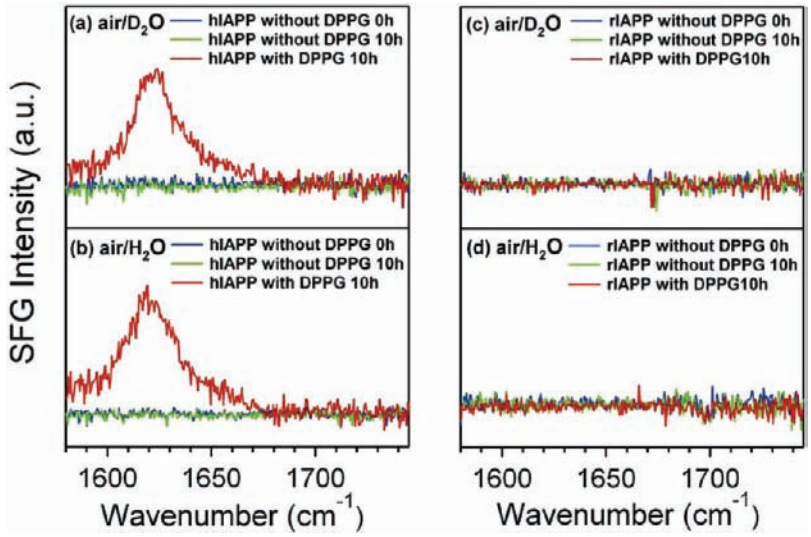

Figure 2. The psp spectra of hIAPP without DPPG ($t = 0$ h and $t = 10$ h) and at $t = 10$ h after addition of DPPG at the (a) air/D_2O and (b) air/H_2O interfaces. The psp spectra of rIAPP without DPPG ($t = 0$ h and $t = 10$ h) and at $t = 10$ h after addition of DPPG at the (c) air/D_2O and (d) air/H_2O interfaces.

amide I band do not change. Because the amide I bands are sensitive to the secondary structure, the results support that DPPG induces changes in the secondary structure of hIAPP, but not rIAPP.

Figure 2 shows the SFG spectra in the amide I region of hIAPP and rIAPP in the presence and absence of DPPG at the air/H_2O and air/D_2O interfaces using the psp polarization that is sensitive only to chirality. Figure 2 a,b shows that the SFG signal can only be observed for hIAPP in the presence, but not absence of DPPG, while Figure 2 c-d shows that no chiral SFG signal can be observed for rIAPP, regardless of the addition of DPPG. These results agree with the results obtained using the ssp polarization and demonstrate again that DPPG can induce changes in the secondary structure of hIAPP, but not rIAPP. The psp spectra of hIAPP at both the air/H_2O and air/D_2O interfaces exhibit a major peak at $\sim$1620 cm^{-1} and a shoulder at $\sim$1660 cm^{-1}. Because the amide I vibrational band at the low-wavenumber region around 1620 cm^{-1} is highly characteristic of β-sheet, the psp spectra indicate that DPPG induces structural changes in hIAPP to form β-sheet structures. Moreover, the 1735-cm^{-1} peak due to the carbonyl group in DPPG that is observed in the ssp spectra (Figure 1) is absent in the psp spectra (Figure 2) even after addition of DPPG. This is not surprising because the carbonyl group of DPPG is achiral and thus silent in the psp spectra. This further indicates that the lipid-induced hIAPP aggregates display chirality. This second-order chiral-optical response could be a highly characteristic optical property for the hIAPP aggregates.

Figure 3 shows the time dependence of the SFG spectra of hIAPP after addition of DPPG using the ssp and psp polarizations at the air/H_2O and air/D_2O interfaces. These time-dependent spectra detail the kinetics of spectral changes between $t = 0$ and 10 h shown in Figure 1 and 2. Because it has been established that the kinetics of the misfolding of amyloid proteins, including hIAPP, is governed by various uncontrollable factors, such as nucleation and agitation, and generally not reproducible, the time-dependent spectra shown in Figure 3 were taken alternately by switching the polarization back and forth between the ssp and psp polarizations to ensure that the same misfolding process was monitored. The ssp spectra (Figure 3 a,b) show that the peak position of the amide I band at the air/D_2O interface gradually shifts from $\sim$1645 to $\sim$1660 cm^{-1} for the air/D_2O interface and from $\sim$1650 to $\sim$1660 cm^{-1} for the air/H_2O interface. Moreover, the psp spectra in Figure 3 c,d show a gradual increase in the intensity of the amide I band at 1620 cm^{-1} at both the air/D_2O, and air/H_2O interfaces. As discussed earlier, the 1620-cm^{-1} peak is characteristic of the β-sheet structures. This result indicates that DPPG triggers a gradual builtup of chiral β-sheet structures in hIAPP. The time-dependent spectra in Figure 3 clearly demonstrate that SFG can be used to probe protein folding at interfaces to yield not only kinetic but also structural information.

Spectral Analysis

To further analyze the secondary structures of hIAPP and rIAPP at both the air/D_2O and air/H_2O interfaces in the presence and absence of DPPG, the psp and ssp spectra are fitted using eq 1. The fittings are presented in Figures 4−6, and the fitting parameters are summarized in the Supporting Information.

Figure 4 shows that the chiral psp spectra of hIAPP in the presence of DPPG ($t = 10$ h) at the air/D_2O and air/H_2O interfaces are fitted into two vibrational bands. The first band centers at 1623 cm^{-1} for the air/D_2O interface and 1622 cm^{-1} for the air/H_2O interface. This low-wavenumber amide I band arises from the antisymmetric stretch of the parallel β-sheet. This vibrational band was observed in the IRRAS and 2D-IR studies and assigned to the parallel β-sheet.[16,17] The second vibrational band is relatively minor and centered at 1657 cm^{-1} for the air/D_2O interface and at 1660 cm^{-1} for the air/H_2O interface; it can be assigned to the symmetric stretch of parallel β-sheet. This assignment is in agreement with the reported simulation showing that the symmetric stretch of stacked parallel β-sheets of hIAPP is at $\sim$1660 cm^{-1}.[16] The spectral analysis suggests that DPPG induces the assembly of chiral structures characteristic of the parallel β-sheet. We speculate that the strong second-order chiral-optical response from the hIAPP aggregates at the antisymmetric stretch frequency of parallel β-sheet at 1620 cm^{-1} could potentially be a highly unique optical property of β-sheet aggregates not only for hIAPP, but also for other amyloid proteins and peptides.

Figure 5 a-b shows the fittings of the ssp spectra of hIAPP in the presence of DPPG ($t = 10$ h). The ssp spectra are fitted

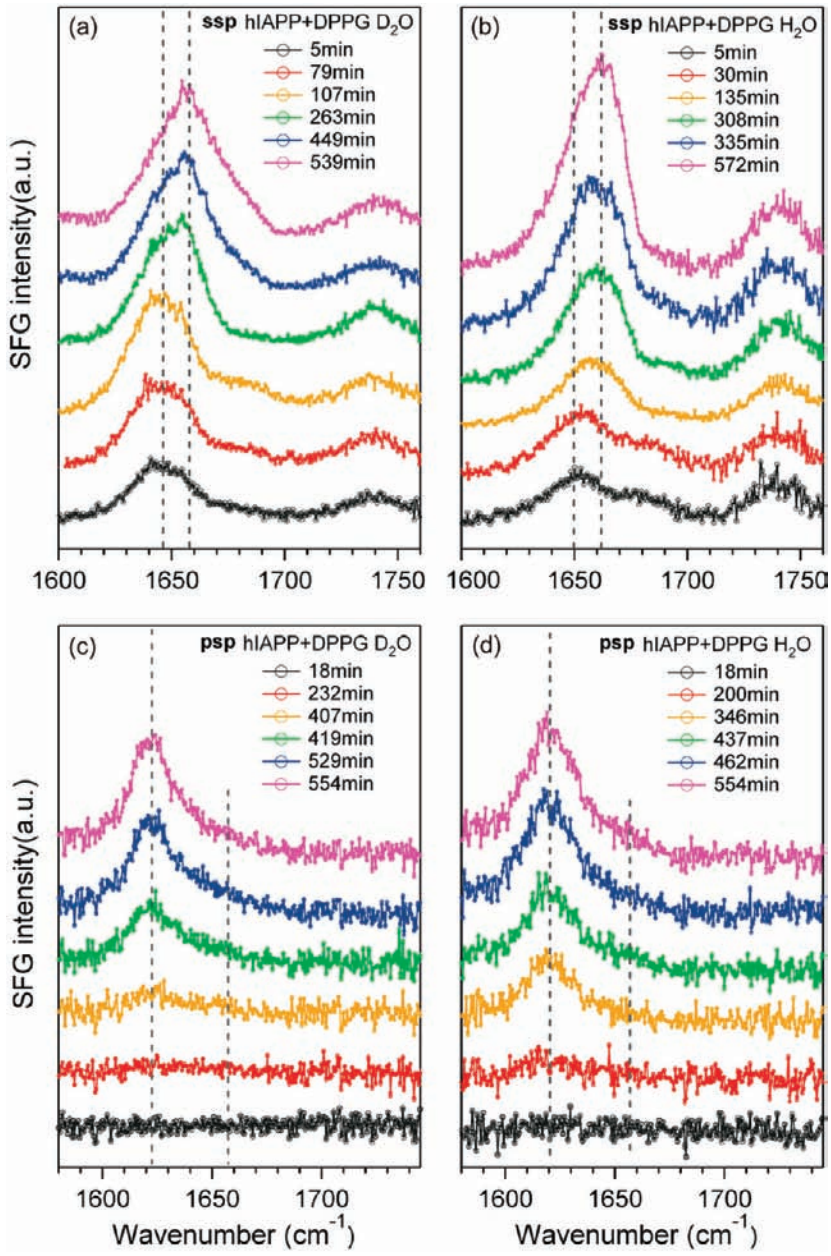

Figure 3. Time-dependent spectra of hIAPP taken using the ssp polarization in the presence of DPPG at the (a) air/D_2O and (b) air/H_2O interfaces. The time-dependent spectra of hIAPP taken using the psp polarization in the presence of DPPG at the (c) air/D_2O and (d) air/H_2O interfaces.

into two amide I bands centered at 1657 cm^{-1} and 1686 cm^{-1} for the air/D_2O interface and 1660 cm^{-1} and 1681 cm^{-1} for the air/H_2O interface, and a carbonyl band centered at 1735 cm^{-1} for the carbonyl group of DPPG at both the air/D_2O and air/H_2O interfaces. The assignments of these peaks are based on three spectroscopic studies. First, NMR studies allowed the establishment of a structural model, in which the misfolded hIAPP contains three kinds of secondary structures, including parallel β-sheets, turn structures, and random coils. Second, the 2D-IR studies showed that the lipid-induced hIAPP aggregates contain the turn and β-sheet structures and the stimulation predicted the amide I bands centered at ~1660 cm^{-1} for the symmetric stretch of parallel β-sheet structures and at ~1680 cm^{-1} for the turn structures. Finally, our fittings of the psp spectra of hIAPP in the presence of DPPG allow the assignment of the ~1620-cm^{-1} and ~1660-cm^{-1} bands to the antisymmetric and symmetric stretch of parallel β-sheet structures, respectively. In the context of these three studies, the 1686-cm^{-1} band for the air/D_2O interface and the 1681-cm^{-1} band for the air/H_2O interface are assigned to turn structures. The 1657-cm^{-1} band for the air/D_2O interface and the 1660-cm^{-1} band for the air/H_2O interface are assigned to the symmetric stretch of the parallel β-sheet.

Figure 5 c-d shows the analysis of the ssp spectra of hIAPP in the absence of DPPG. The spectra exhibit a peak centered at ~1650 cm^{-1}. The amide I bands center around 1650 cm^{-1} are often assigned to the α-helical and/or random-coil structures.[24] As shown by previous vibrational studies of proteins, an attempt to distinguish between the random coil and α-helical structures is often not definitive because the amide I bands of these secondary structures are clustered in the 1640−1660 cm^{-1} region.[24] Consequently, the spectra are unarbitrarily fitted into a single vibrational band centered at 1647 cm^{-1} for the air/D_2O interface and 1650 cm^{-1} for the air/H_2O interface. These fittings

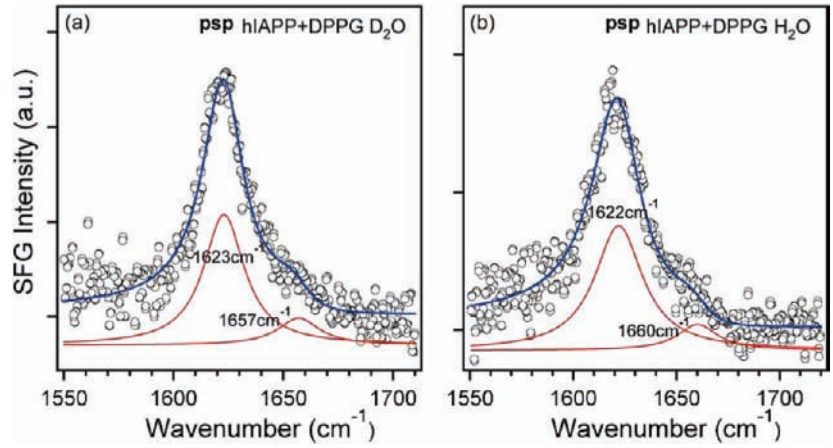

Figure 4. The fitting of the psp spectra of hIAPP in the presence of DPPG at the (a) air/D_2O and (b) air/H_2O interfaces. The 1623- and 1622-cm^{-1} peaks are assigned to the antisymmetric stretch of the parallel β-sheet structure and the 1657- and 1660-cm^{-1} peaks are assigned to the symmetric stretch of the β-sheet structure.

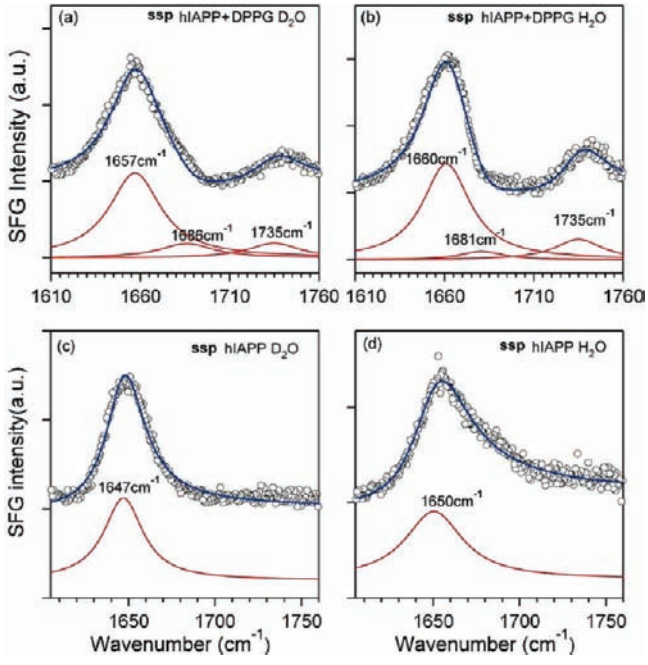

Figure 5. The fitting of the ssp spectra of hIAPP in the presence of DPPG at the (a) air/D_2O and (b) air/H_2O interfaces. The 1657- and 1660-cm^{-1} peaks are assigned to β-sheet structures and the 1686- and 1681-cm^{-1} peaks are assigned to turn structures. The fitting of the ssp spectra of hIAPP in the absence of DPPG at the (c) air/D_2O and (d) air/H_2O interfaces. The 1647- and 1650-cm^{-1} peaks are assigned to β-helical structures with some contribution from random coil structures.

are interpreted based on two previous studies. First, Miranker and co-workers preformed helical-wheel analysis of hIAPP and found that amino acid (a.a.) 8−27 in hIAPP can form amphiphilic α-helical structures.[14] Similarly, Langen and co-worker used electron paramagnetic resonance (EPR) spectroscopy to study hIAPP and proposed that the N-terminus (a.a. 1−8) and C-terminus (a.a. 28−37) are likely to form random coils to either side of the amphiphilic α-helical structure (a.a. 8−27).[26] Hence, it is not surprising that hIAPP is surface active and stable at the air/water interface because hIAPP can be energetically driven to the air/water interface by displaying the hydrophobic side and hydrophilic side of the helical segment to the air phase and water phase, respectively. Consequently, we attribute the ∼1650 cm^{-1} peak to the α-helical structure. It is also possible that this peak contains some contribution from random coil at the N- and C-termini. However, the contribution is expected to be small because the random-coil regions of hIAPP are hydrophilic and likely to be submerged in water.

Finally, Figure 6 shows the fitting of the ssp spectra of rIAPP. The amide I vibrational band is fitted to a single peak centered at 1639 cm^{-1} for the air/D_2O interface and 1647 cm^{-1} for the air/H_2O interface. It is known that hIAPP and rIAPP differ by six amino acids. Rammamoorthy et al. performed NMR studies on both rIAPP and hIAPP.[27] They found that both hIAPP and rIAPP form similar α-helical structures; however, compared to the helix formed by hIAPP, the helix formed by rIAPP is shorter. In addition, a previous CD study also suggested that rIAPP has less propensity to form α-helical structures than hIAPP.[14] Therefore, the random-coil structure is likely to have a relatively larger contribution to the amide I peak in the rIAPP spectra (Figure 6) compared to that in the hIAPP spectra (Figure 5). Indeed, the isotopic shift for rIAPP from 1639 to 1647 cm^{-1} is bigger than that for hIAPP from 1647 to 1650 cm^{-1} (Figure 5 c,d) We speculate that the larger isotopic shift observed for rIAPP could be due to that rIAPP adopts more random coil structures than hIAPP does at the air/water interface and that random-coil structures exhibit larger isotope shifts in the amide I region as demonstrated by previous studies.[24]

Discussion

Summary. We monitored the SFG spectra of hIAPP and rIAPP in the amide I region in the presence and absence of DPPG at the air/H_2O and air/D_2O interfaces. We carried out the experiments using the ssp polarization, which is sensitive to achiral structures, and the psp polarization, which is sensitive to chiral structures. The ssp spectra of hIAPP exhibit changes in both peak position and shape over a period of 10 h in the presence but not absence of DPPG, while the ssp spectra of rIAPP do not undergo such changes either in the presence or in the absence of DPPG. Moreover, the chiral psp signal cannot be detected from rIAPP regardless of the presence of DPPG and cannot be detected from hIAPP unless DPPG is added.

(26) Apostolidou, M.; Jayasinghe, S. A.; Langen, R. *J. Biol. Chem.* **2008**, *283*, 17205–17210.

(27) Nanga, R.; Prakash, Ravi; Brender, J. R.; Xu, J.; Veglia, G.; Ramamoorthy, A. *Biochemistry* **2008**, *47*, 12689–12697.

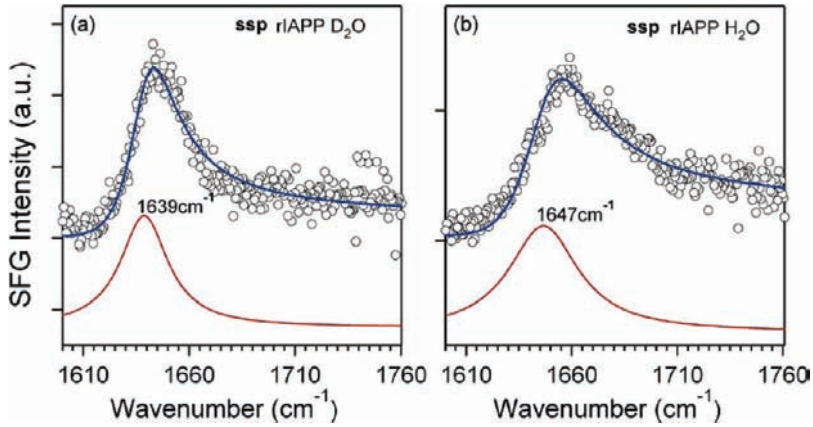

Figure 6. The fitting of the ssp spectra of rIAPP in the absence of DPPG at the (a) air/D_2O and (b) air/H_2O interfaces. The 1639- and 1647-cm^{-1} bands are assigned to β-helical structures, with some contribution from random coil structures.

Furthermore, the chiral SFG signal is centered at ~1620 cm^{-1}, a characteristic amide I frequency for the antisymmetric stretch of the parallel β-sheet structures. Our results agree with previous *in vitro* biophysical studies of the misfolding process of hIAPP using a variety of spectroscopic techniques, including fluorescence,[12,15,28] circular dichorism,[12,14] NMR,[18,29,30] infrared,[16,17,31−33] and Raman spectroscopies.[34] These studies support the conclusion that the interaction between the membrane and hIAPP triggers the misfolding of hIAPP and leads to the formation of highly ordered parallel β-sheet structures. The agreement of our results with these studies further underlines the applicability of SFG in probing the kinetics of protein conformational changes in peptides and proteins.

Chiral-Optical Response of SFG and Amyloidgenesis. The chiral-optical response of SFG provides the possibility to formulate a new approach for investigating amyloidgenesis, which is central in many disorders such as Alzheimer's disease, Parkinson's disease, Huntington's disease, etc. As demonstrated in our experiments, the second-order chiral-optical SFG response from the hIAPP aggregates is background-free (Figure 2), which is advantageous for *in situ* detection with high sensitivity. Recently, Chen and co-workers observed chiral SFG signal at the polystyrene/liquid interface using the psp polarization from the tachyplesin I peptide adopting an antiparallel β-sheet structure, which is formed by intramolecular hydrogen bonds.[35] In our studies, we observed the chiral SFG signal using the same polarization corresponding to the formation of parallel β-sheet structures, which are formed by intermolecular hydrogen bonds that are responsible for assembling hIAPP into supramolecular structures. Simpson and co-workers have recently developed a theory of SFG observed from chiral molecular entities and demonstrated that chiral SFG can be generated from the macromolecular orientation of uniaxial systems without the need for multiple coupled oscillators or even a chiral chromophore[36−38] and several research groups have observed that the chiral orientation of individual molecules in supramolecular assemblies could dominate the chiral-optical responses.[22,39] On the basis of these theoretical and experimental developments, we speculate that the psp signal of hIAPP originates from the assembling of individual hIAPP molecules into a supramolecular chiral architecture. Although this remains to be confirmed, our observed second-order chiral-optical response at the amide I frequency of β-sheet could be a unique optical property of amyloid, hence revealing the potential of utilizing this property for *in vivo* detection of amyloids.

Molecular Model of hIAPP at the Air/Water Interface. To further analyze the secondary structures of hIAPP and rIAPP, we fitted the SFG spectra into various amide I vibrational bands. In the absence of DPPG, the ssp spectra are fitted into single peaks centered at ~1650 cm^{-1}, which contain contributions from both the random-coil and α-helical structures. In the presence of DPPG, the ssp spectra of hIAPP are fitted into two amide I bands at ~1660 and ~1685 cm^{-1} assigned to the symmetric stretch of the β-sheet and turn structures, respectively, while the psp spectra are fitted into two amide I bands centered at ~1623 and ~1660 cm^{-1} and assigned to the antisymmetric and symmetric stretch of the β-sheet, respectively. It is to be noted that the antisymmetric stretch of the parallel β-sheet at ~1623 cm^{-1} observed in the psp spectra is not observed in the ssp spectra. This is not surprising because the long axis of the β-sheet formed by hIAPP could be in parallel to the air/water interface as suggested by previous IRRAS studies.[17] Thus, the transition dipole of the antisymmetric stretch of the amide I mode (~1620 cm^{-1}) lies flat in the surface plane, leading to a very weak SFG signal. Consequently, we propose that hIAPP adopts the α-helical and random-coil structures at the air/water interface in the absence of DPPG. Upon interactions with the lipid molecules at the air/water interface, hIAPP gradually folds into the parallel multistranded β-sheets, together with the turn structures between the strands of β-sheets and the long axis of

(28) Knight, J. D.; Miranker, A. D. *J. Mol. Biol.* **2004**, *341*, 1175–1187.
(29) Williamson, J. A.; Loria, J. P.; Miranker, A. D. *J. Mol. Biol.* **2009**, *393*, 383–396.
(30) Brender, J. R.; Durr, U. H. N.; Heyl, D.; Budarapu, M. B.; Ramamoorthy, A. *Biochim. Biophys. Acta, Biomembr.* **2007**, *1768*, 2026–2029.
(31) Tenidis, K.; Waldner, M.; Bernhagen, J.; Fischle, W.; Bergmann, M.; Weber, M.; Merkle, M. L.; Voelter, W.; Brunner, H.; Kapurniotu, A. *J. Mol. Biol.* **2000**, *295*, 1055–1071.
(32) Shim, S. H.; Gupta, R.; Ling, Y. L.; Strasfeld, D. B.; Raleigh, D. P.; Zanni, M. T. *Proc. Natl. Acad. Sci. U.S.A.* **2009**, *106*, 6614–6619.
(33) Strasfeld, D. B.; Ling, Y. L.; Gupta, R.; Raleigh, D. P.; Zanni, M. T. *J. Phys. Chem. B* **2009**, *113*, 15679–15691.
(34) Xu, M.; Shashilov, V.; Lednev, I. K. *J. Am. Chem. Soc.* **2007**, *129*, 11002–11003.
(35) Wang, J.; Chen, X. Y.; Clarke, M. L.; Chen, Z. *Proc. Natl. Acad. Sci. U.S.A.* **2005**, *102*, 4978–4983.
(36) Simpson, G. J. *J. Chem. Phys.* **2002**, *117*, 3398–3410.
(37) Moad, A. J.; Simpson, G. J. *J. Phys. Chem. B* **2004**, *108*, 3548–3562.
(38) Haupert, L. M.; Simpson, G. J. *Annu. Rev. Phys. Chem.* **2009**, *60*, 345–365.
(39) Nagahara, T.; Kisoda, K.; Harima, H.; Aida, M.; Ishibashi, T. A. *J. Phys. Chem. B* **2009**, *113*, 5098–5103.

the β-sheets aligned parallel to the air/water interface. These analyses illustrate that the optical response of vibrational modes to various polarization settings in the SFG experiments can provide insight into molecular structures and orientations at interfaces.

Advantages of SFG. In probing the kinetics of conformational changes of proteins, SFG has several advantages over conventional techniques, such as NMR, EPR, CD, and fluorescence spectroscopy. Although NMR can provide detailed structural information, the method is generally not applicable for kinetic studies and requires a large amount of samples. Although fluorescence is an excellent technique in probing the kinetics of the folding process, the spectroscopic signal is generally scarce in structural information. CD allows studies of changes in secondary structure, but the concentration of the samples needs to be high, and the fundamental basis for the CD response from amyloid fibrils has not been fully established.[14,15] EPR can yield important structural information, but it introduces molecular perturbation by introducing cysteine mutations and electron spin labels.[40] By contrast, several characteristics of SFG enable it to supply information not obtained by these techniques. First, SFG is surface specific. At most, a monolayer of sample is needed for the SFG experiments. In our experiments, 4 μg of sample was needed for each spectrum, which can be further reduced. Second, SFG can be used to probe the amide I vibrational structure of the peptide without using a spectroscopic label. Finally, being an optical technique, SFG is useful *in situ* for monitoring the conformational changes of proteins and yielding kinetic information.

SFG Complementary to Raman and Infrared Spectroscopy. SFG can be complementary to other types of vibrational spectroscopy, including Raman and FTIR spectroscopy. Because SFG is a second-order optical technique that is sensitive only to the molecules at interface, unlike reflection absorption infrared spectroscopy or surface-enhanced Raman spectroscopy, SFG does not rely on detection geometry to suppress bulk signals or metal substrate to enhance surface signals. Being sensitive to the vibrational modes that are both infrared- and Raman-active, SFG suffers less from the spectral background of solvent and is able to provide a wider spectral window to investigate vibrational structures of bioactive molecules upon interaction with proteins. In probing the amide I structure, SFG does not suffer from significant background of the bending modes of water as demonstrated in the ssp and psp measurements, and hence results in higher sensitivity in the amide I region. In contrast to Raman and IR spectroscopy, SFG is a coherent optical technique, and the vibrational spectra taken using various input and output polarizations can reveal additional molecular information.[41] For example, the phase and ratio of different nonlinear susceptibilities can reveal molecular orientation,[19,42,43] and the chiral hyperpolarizibility can probe chirality of vibrational structures.[22,35] These characteristics make SFG a complementary vibrational spectroscopy for investigating structures and functions of proteins, peptides, and other biomolecules at interfaces.

Acknowledgment. We thank Professor Andrew Miranker (Yale University) for providing the rIAPP sample for the pilot study and Dr. Jian Liu for assistance at the early stage of this work. We thank Spectroscopy Society of Pittsburgh for the Starter Grant Award to support this work.

Supporting Information Available: The table of fitting parameters for the spectra analysis is given in Supporting Information. This information is available free of charge via the Internet at http://pubs.acs.org.

JA909546B

(40) Apostolidou, M.; Jayasinghe, S.; Langen, R. *Biophys. J.* **2005**, *88*, 422A–422A.

(41) Hirose, C.; Akamatsu, N.; Domen, K. *Appl. Spectrosc.* **1992**, *46*, 1051–1072.

(42) Nguyen, K. T.; Le Clair, S. V.; Ye, S. J.; Chen, Z. *J. Phys. Chem. B* **2009**, *113*, 12169–12180.

(43) Ye, S.; Nguyen, K. T.; Le Clair, S. V.; Chen, Z. *J. Struct. Biol.* **2009**, *168*, 61–77.